



Fermi National Accelerator Laboratory

FN-379
8050.000

SKIN EFFECT IN ELECTRICALLY PULSED CYLINDRICAL CONDUCTORS
USED AS FOCUSING DEVICES

A. J. Lennox

January 1983



Skin Effect in Electrically
Pulsed Cylindrical Conductors
Used as Focusing Devices

A.J. Lennox

January 28, 1983

Introduction

Recently there has been some interest in using the magnetic field inside a current-carrying cylindrical conductor to focus particle beams.¹⁻⁸ Applications include focusing targets and lithium lenses. The calculations described in this report were done in connection with the design of a lithium lens to focus antiprotons just downstream of the production target for the $\bar{p}p$ collider at Fermilab. However, many of the results are generally applicable for any pulsed cylindrical conductor.

For the simple case of a cylindrical conductor of radius r_0 carrying total current I with uniform current density \vec{J} the magnetic induction \vec{B} inside the conductor can be found from Ampere's Circuital Law. Using the International System of units (SI) this law can be written

$$\oint \vec{B} \cdot d\vec{s} = \mu \int \vec{J} \cdot d\vec{a}$$

where the magnetic permeability μ for a linear material is given by

$\mu = \mu_r \mu_0$, with μ_r being relative permeability and with $\mu_0 = 4\pi \times 10^{-7}$ henry/meter. Applying the Law results in the expression

$$B(r) = \frac{\mu I}{2\pi} \frac{r}{r_0^2} \quad (1)$$

or

$$B(r) = B(r_0) \frac{r}{r_0} \quad (2)$$

where $B(r_0)$ is the value of the field at the surface of the cylinder. Since the material is assumed to be linear ($\vec{B} = \mu \vec{H}$) equation (2) can also be written

$$H(r) = H(r_0) \frac{r}{r_0}$$

For many applications the Joule heating from direct current is prohibitively large. To minimize heating these devices are often pulsed with a sine-like unipolar pulse whose width $\tau/2$ is small compared to the time between pulses. For the pulsed device an expression describing the magnetic intensity \vec{H} as a function of radial position in the conductor and time can be derived by solving Maxwell's equations with appropriate boundary conditions. A solution applicable to a pulsed lithium lens with $I = I_0 \sin \omega t$ for $0 < t < \pi/\omega$ is given in reference 8. This paper assumes the cylindrical conductor is a component in an RLC circuit and has a pulse

shape modified by a damping factor $e^{-\alpha t}$ where $\alpha = R/2L$. The mathematical description of the pulse form is $I = I_0 e^{-\alpha t} \sin \omega t$ for $0 < t < \pi/\omega$ where $\omega = 2\pi/\tau$ and $I = 0$ between pulses.

The paper is presented in three parts. In part A an expression for $\vec{H}(r,t)$ is derived and the time during the pulse corresponding to maximum linearity is calculated. In part B an expression for the current density J_z is derived and a method for measuring J_z at the surface of the conductor is discussed. Part C describes Joule heating, including the radial dependence of temperature and the total heat deposited per pulse.

A. Magnetic Field Intensity in a Pulsed Conductor

This section describes a derivation of an expression for the magnetic field intensity \vec{H} in a pulsed cylindrical conductor. The time at which the field is most linear and the gradient at that time are also calculated.

Assuming that the displacement current is negligible the appropriate Maxwell's equations are

$$\vec{J} = \vec{\nabla} \times \vec{H} \quad (3)$$

$$\vec{J} = \sigma \vec{E} \quad (6)$$

$$\vec{\nabla} \times \vec{E} = -\frac{\partial \vec{B}}{\partial t} \quad (4)$$

$$\vec{B} = \mu \vec{H} \quad (7)$$

$$\vec{\nabla} \cdot \vec{H} = 0 \quad (5)$$

where σ is the conductivity and t is the time.

Taking the curl of both sides of (3) and using (6) gives

$$\vec{\nabla} \times (\vec{\nabla} \times \vec{H}) = \vec{\nabla} \times \sigma \vec{E} \quad (8)$$

Using appropriate vector identities and (4), equation (8) becomes

$$\vec{\nabla}^2 \vec{H} = \sigma \mu \frac{\partial \vec{H}}{\partial t} \quad (9)$$

Assuming that the cylinder is coaxial with the z axis, that \vec{H} has only an azimuthal (ϕ) component and that the magnitude of \vec{H} depends only on r and t, equation (9) simplifies to

$$\frac{\partial^2 H}{\partial r^2} + \frac{1}{r} \frac{\partial H}{\partial r} - \frac{H}{r^2} = \sigma \mu \frac{\partial H}{\partial t} \quad (10)$$

where H is the azimuthal component of \vec{H} . The boundary conditions are

$$H(r,0) = 0; H(0,t) = 0 \quad (11)$$

$$\text{and } H(r_0,t) = H_0 e^{-\alpha t} \text{Re}\{i e^{-i\omega t}\} \quad (12)$$

where H_0 is the maximum value of H for an undamped pulse. The problem is inhomogeneous because the right-hand-side of (12) is nonzero. A general solution to (10) can be found by solving the homogeneous problem with $H(r_0,t) = 0$ and then adding a particular solution satisfying (12). The homogeneous problem is an eigenvalue problem which is solved using the separation of variables technique. A solution to the homogeneous problem is

$$H_h(r,t) = \sum_j a_j J_1(\lambda_j r) e^{-\lambda_j^2 t / \sigma \mu} \quad (13)$$

Where $J_1(x)$ is a first order Bessel function with a real argument, $\lambda_j r_0$ is a root of $J_1(x) = 0$ and the a_j are coefficients to be determined from the boundary conditions at $t = 0$.

A particular solution is found by separating variables and assuming a damped sinusoidal time dependence. Thus

$$H_p(r,t) = \mathcal{H}(r) T(t) \quad (14)$$

where $T = Ce^{-\gamma t}$ and $\gamma = \alpha + i\omega$. This leads to the equation

$$\frac{d^2 H_p}{dr^2} + \frac{1}{r} \frac{dH_p}{dr} - \frac{H_p}{r^2} = -\beta^2 H_p \quad (15)$$

where $\beta^2 = \sigma \mu \gamma = \sigma \mu (\alpha + i\omega)$. Letting $\sigma \mu \omega = 2/\delta^2$, the expression $i\omega \sigma \mu$ becomes $2i/\delta^2$. The variable δ is commonly called the skin depth. Thus β^2 can be expressed in terms of the attenuation coefficient α and the skin depth:

$$\beta^2 = \sigma \mu \alpha + 2i/\delta^2$$

Equation (15) takes the form

$$\frac{d^2 H_p}{dr^2} + \frac{1}{r} \frac{dH_p}{dr} + \left(\beta^2 - \frac{1}{r^2} \right) H_p = 0 \quad (16)$$

This is a Bessel equation having the solution

$$H(r) = AJ_1(\beta r) \quad (17)$$

where $J_1(\beta r)$ is a first order Bessel function of complex argument. Applying the boundary condition (12) to (17) and substituting the result into (14) gives the particular solution

$$H_p(r, t) = H_0 \frac{J_1(\beta r)}{J_1(\beta r_0)} i e^{-\gamma t} \quad (18)$$

A general solution to (10) is the sum of expressions (13) and the real part of (18).

$$H(r, t) = H_0 \operatorname{Re} \left\{ \frac{i J_1(\beta r)}{J_1(\beta r_0)} e^{-\gamma t} \right\} + \sum_j a_j J_1(\lambda_j r) e^{-\lambda_j^2 t / \sigma \mu} \quad (19)$$

The a_j coefficients are evaluated using the boundary condition $H(r, 0) = 0$.

At $t = 0$, equation (19) becomes

$$0 = -H_0 \operatorname{Im} \frac{J_1(\beta r)}{J_1(\beta r_0)} + \sum_j a_j J_1(\lambda_j r).$$

Applying the orthogonality properties of $J_1(\lambda_j r)$ leads to

$$a_j = \frac{2H_0}{r_0^2 [J_2(\lambda_j r_0)]^2} \int_0^{r_0} r J_1(\lambda_j r) \operatorname{Im} \frac{J_1(\beta r)}{J_1(\beta r_0)} dr.$$

Evaluating the integral gives

$$a_j = -4H_0 \frac{r_0^2}{\delta^2} \frac{\lambda_j r_0}{[(\lambda_j^2 - \sigma\mu\alpha)r_0^2]^2 + 4(r_0/\delta)^4} \frac{1}{J_0(\lambda_j r_0)}$$

The time dependence of the penetration of the field into the conductor is illustrated in Figure 1 which shows H/H_0 vs r/r_0 for various values of ωt with $\delta/r_0 = 0.5$. Fig. 2 presents the same information in a different way, with H/H_0 plotted vs ωt for various values of r/r_0 .

The time at which the field is most linear depends on δ/r_0 and α . This time can be calculated as follows.⁹

$$(\Delta H)^2 = [H(r,t) - G(t) r]^2 \quad (20)$$

is a measure of the deviation of the field from linearity and the expectation value of $(\Delta H)^2$ is

$$\langle (\Delta H)^2 \rangle = \frac{1}{\pi r_0^2} \int_0^{2\pi} \int_0^{r_0} (\Delta H)^2 r dr d\phi \quad (21)$$

The value of G corresponding to a minimum expectation value is found by solving the equation

$$\frac{\partial}{\partial G} \langle (\Delta H)^2 \rangle = 0$$

or

$$-\frac{4}{r_0^2} \int_0^{r_0} r^2 H(r,t) dr + \frac{4G}{r_0^2} \int_0^{r_0} r^3 dr = 0 \quad (22)$$

from which

$$G = \frac{4}{r_o^2} H_o \operatorname{Re} \left\{ \frac{ie^{-\gamma t}}{\beta} \frac{J_2(\beta r_o)}{J_1(\beta r_o)} \right\} - \sum_j \frac{a_j}{\lambda_j} J_o(\lambda_j r_o) e^{-\lambda_j^2 t / \sigma \mu} \quad (23)$$

A measure of the goodness of fit to a straight line is found by substituting (23) into (21) and performing the integration. Some results are presented in Fig. 3 which shows the deviation from linearity as a function of time for $\delta/r_o=0.5$ with $\alpha=0$ and $\alpha=1000 \text{ sec}^{-1}$. The case where $\delta/r_o=1.0$ is shown for comparison. The results of evaluating (21) for various values of δ/r_o are given in Fig. 4 which shows the time corresponding to maximum linearity vs δ/r_o . For $\delta/r_o \geq 0.7$ the summation over j in (23) becomes negligible and one can derive an expression for $(\omega t)_\ell$, the time corresponding to maximum linearity as follows. Substituting the first term of (23) into (21) leads to the expression

$$\langle (\Delta H)^2 \rangle = \frac{H_o^2}{r_o^2} e^{-2\alpha t} \int_0^r \left[-\operatorname{Re} f^2 e^{-2i\omega t} + ff^* \right] r dr \quad (24)$$

where

$$f = \frac{J_1(\beta r)}{J_1(\beta r_o)} - \frac{4r}{r_o^2 \beta} \frac{J_2(\beta r_o)}{J_1(\beta r_o)}$$

The optimum value of ωt is found by differentiating (24) with respect to ωt and setting the derivative equal to zero. This leads to the result

$$\tan 2(\omega t)_\ell = \frac{\int_0^{r_0} \text{Im} f^2 r dr}{\int_0^{r_0} \text{Re} f^2 r dr} \quad (25)$$

The error introduced by this approximation increases as δ/r_0 decreases, ranging from 2° at $\delta/r_0 = 0.5$ to 8° at $\delta/r_0 = 0.3$. The values shown in Fig. 4 were calculated using the complete expression (23) rather than the approximation. Fig. 5 shows H/H_0 vs r/r_0 when the field is most linear.

B. Current Density in a Pulsed Cylindrical Conductor

An expression for the current density may be derived using Maxwell's equation $\vec{J} = \vec{\nabla} \times \vec{H}$. The curl of the expression for $\vec{H}(r,t)$ given in (19) has only a z component

$$J_z(r,t) = H_0 \text{Re} \left[i e^{-\gamma t} \frac{\beta J_0(\beta r)}{J_1(\beta r_0)} \right] + \sum_j a_j \lambda_j J_0(\lambda_j r) e^{-\lambda_j^2 t / \sigma \mu} \quad (26)$$

Fig. 6 shown J_z vs r/r_0 for various times during the pulse. Fig. 7

contains the same information with J_z vs ωt for various values of r/r_0 . The curve describing J_z at the surface of the conductor vs ωt is of particular interest because it is related to the potential difference between two points on the surface of the conductor via the equation $V = \int \vec{E} \cdot d\vec{\ell} = \rho \int \vec{J} \cdot d\vec{\ell}$ where ρ is the electrical resistivity of the conductor. Consider a line segment of length L , parallel to the axis of the cylinder and having as its endpoints two points on the surface of the cylinder. The potential difference between these points at time t is $L\rho J_z(r_0, t)$. Measurement of this potential difference provides a sensitive test of whether or not the actual device is producing the expected field.¹⁰

C. Joule Heating in a Pulsed Cylindrical Conductor

An expression for heating due to ohmic losses can be found by evaluating the integral $\int \vec{J} \cdot \vec{E} dt dV$. This will be done assuming constant resistivity during the pulse and then a method for taking into account a changing resistivity will be given. The radial distribution of heat is given by

$$q_o(r) = \rho \int_0^{\pi/\omega} J_z^2 dt$$

Using (26) for J_z one obtains

$$\begin{aligned} q_o(r) = & \frac{H_0^2}{4\sigma} \left[\operatorname{Re} \left(\frac{\beta^2 J_0^2(\beta r)}{\gamma J_1^2(\beta r_0)} \right) - \frac{1}{\alpha} \left| \frac{\beta J_0(\beta r)}{J_1(\beta r_0)} \right|^2 \right] (e^{-2\alpha\pi/\omega} - 1) \\ & + 2 \frac{H_0}{\sigma} \operatorname{Re} \left[i\beta \frac{J_0(\beta r)}{J_1(\beta r_0)} \sum_j \frac{a_j \lambda_j J_0(\lambda_j r)}{\gamma + \lambda_j^2/\sigma\mu} \right] (1 + e^{-\pi(\alpha + \lambda_j^2/\sigma\mu)/\omega}) \\ & + \mu \sum_j \sum_n \frac{a_j a_n \lambda_j \lambda_n}{\lambda_j^2 + \lambda_n^2} J_0(\lambda_j r) J_0(\lambda_n r) (1 - e^{-\pi\delta^2(\lambda_j^2 + \lambda_n^2)/2}) \end{aligned}$$

(27)

The units for q_0 are Joules/m³ and the temperature rise $\Delta T(r)$ can be calculated from (27) by dividing $q_0(r)$ by the heat capacity c . The total heat generated per pulse unit length is given by

$$Q_0 = \int_0^{r_0} q_0(r) 2\pi r dr$$

The result of this integration is

$$\begin{aligned} Q_0 = & \frac{H_0^2 \pi (\beta r_0)^2}{4\sigma \gamma} \left(\frac{J_0^2(\beta r_0)}{J_1^2(\beta r_0)} + 1 \right) (e^{-2\pi\alpha/\omega} - 1) \\ & - \frac{H_0^2 \pi r_0}{\sigma} \frac{\beta\beta^*}{\beta^2 - \beta^{*2}} \frac{e^{-2\pi\alpha/\omega} - 1}{\alpha} \left\{ 1 + \operatorname{Im} \left(\frac{\beta J_0^*(\beta r_0)}{J_1^*(\beta r_0)} \right) \right\} \\ & + \frac{4\pi H_0 r_0}{\sigma} \operatorname{Re} \left\{ i\beta^2 \sum_j a_j \lambda_j \frac{J_0(\lambda_j r_0)}{\beta^2 - \lambda_j^2} \frac{1 + e^{-\pi(\alpha + \lambda_j^2/\sigma\mu)/\omega}}{\gamma + \lambda_j^2/\sigma\mu} \right\} \end{aligned} \quad (28)$$

Both (27) and (28) were derived assuming a constant resistivity. An approximation which can be used to take into account the temperature dependence of resistivity is given by Knoepfel.¹¹ The resistivity can be parameterized by

$$\rho = \rho_0(1+bQ)$$

where b is the heat factor and Q the increase of heat content relative to 0°C . In the solid phase

$$Q = c_v \Delta T.$$

In the case of lithium, one uses the slope of a ρ vs T curve and the value $c_v = 2.0 \times 10^6 \text{ Jm}^{-3}/^\circ\text{C}$ to calculate $b = 2.4 \times 10^{-9} \text{ m}^3/\text{J}$. If Q_0 is the heat per unit volume calculated in (28) then the "corrected" value is

$$Q = \frac{e^{bQ_0} - 1}{b} \quad (29)$$

Fig. 8 shows the total heat deposited during a single pulse of a 1 cm radius lithium cylinder with $I_0 = 500 \text{ kA}$. The dashed curve is the result of evaluating (28) and the solid curve includes the correction specified in (29). Fig. 9 shows the radial distribution of heating including the correction for changing resistivity.

D. Some Conclusions

In designing a focusing target or a lithium lens it is necessary to optimize several parameters. Linearity is improved by increasing the pulse length but the longer the pulse the greater the demands on the cooling

system. For lithium, which melts at 180°C one must decide whether to try to prevent melting or to operate with the lithium in the liquid state. The volume expansion upon melting stresses the vessel so an effort should be made to keep the lithium in one state or the other. For δ/r_0 values around 0.5 the maximum linearity occurs 20-30° after the current peak (Figs. 2 and 4). To achieve the required gradient at that time during the pulse, the peak current may have to be scaled up. Thus, increased linearity requires increased power and heat load. Finally, the optimization for linearity was calculated assuming a uniform distribution of particles impinging on the lens. For a focusing target where the incident particles are concentrated on the axis the optimum time could be different from the one given here.

References & Footnotes

1. B.F. Bayanov, J.N. Petrov, G.I. Sil'vestrov, J.A. MacLachlan, and G.L. Nicholls, "A Lithium Lens for Axially Symmetric Focusing of High Energy Particle Beams", Nucl. Inst. and Meth. Vol. 190, 9 (1981).
2. L.N. Blumberg and A.E. Webster, "Secondary Yield Enhancement from Current Carrying Target", IEEE Transactions on Nuclear Science, Vol. NS-24, No. 3, 1539 (1977).
3. G.I. Budker et al., Proc. V. Sov. Nat'l. Conf. on Part. Accel., V. II, Dubna, 299 (1976).
4. D. Cline and F. Mills, "Exploding Wire Lens for Increased \bar{p} Yield", Fermilab \bar{p} Note No. 7, January 1979 (unpublished).
5. J.A. MacLachlan, "Current Carrying Targets and Multitarget Arrays for High Luminosity Secondary Beams", Fermilab FN-334, 8055.000, April 1982.
6. C. Rubbia, "Focusing Antiprotons Inside the Production Target", Fermilab \bar{p} Note No. 12, January 1979 (unpublished).

7. L.C. Teng, "Study of Current Carrying \bar{p} Production Target", \bar{p} Note No. 14, February 1979 (unpublished).
8. T.A. Vsevolozhskaya, M.A. Lyubimova, and G.I. Sil'vestrov, "Optical Properties of Cylindrical Lenses", Sov. Phys. Tech. Phys. Vol. 20, No. 12, 1556 (1977).
9. This approach to the problem is taken from reference 8.
10. For a brief description of an actual measurement using a tantalum cylinder see Fermilab \bar{p} Note No. 262, "A Short Analysis of the Voltage Observed on the Surface of the Tantalum Dummy Lens", A.J. Lennox, January 1983 (unpublished).
11. H. Knoepfel, Pulsed High Magnetic Fields , North-Holland Publishing Company, London, 1970, p. 88.

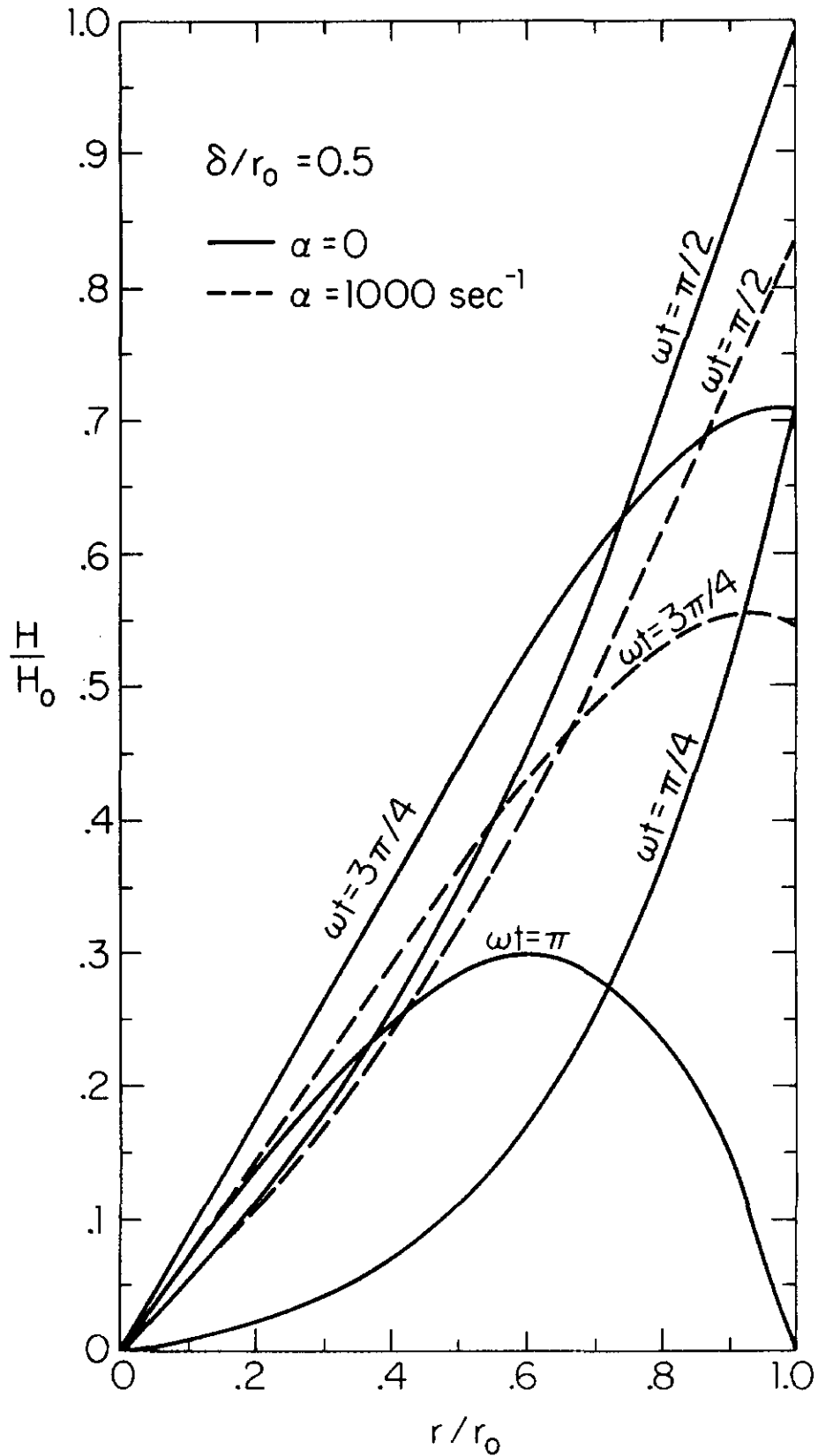


Fig. 1 Magnetic intensity vs radius at several times during the pulse. H_0 has units amp/meter and is the value of H corresponding to I_0 in the expression $I = I_0 e^{-\alpha t} \sin \omega t$. For an undamped pulse it is the maximum value of H at the surface of the cylinder.

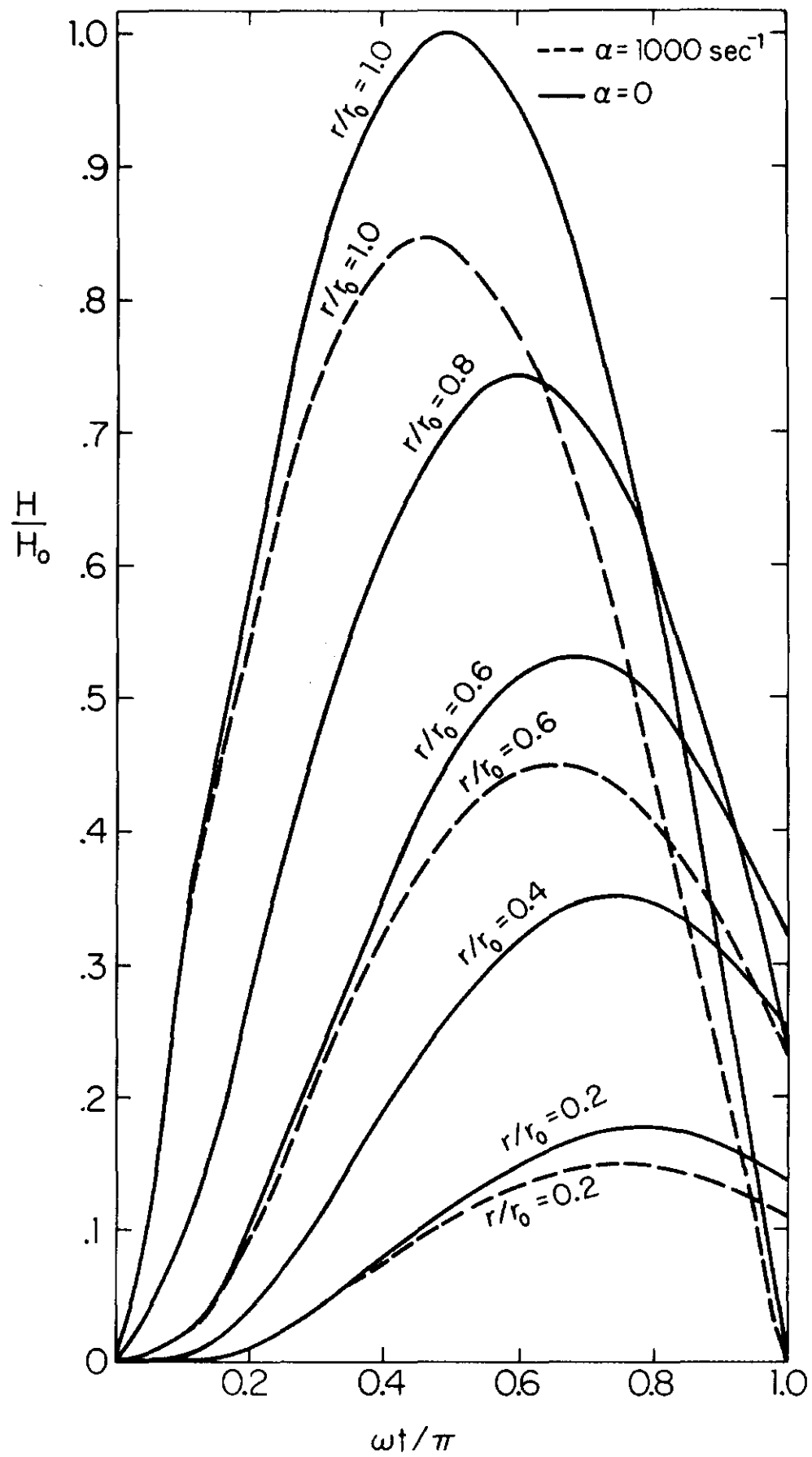


Fig. 2 Magnetic intensity vs time for various distances from the axis. This figure contains the same information as Fig. 1.

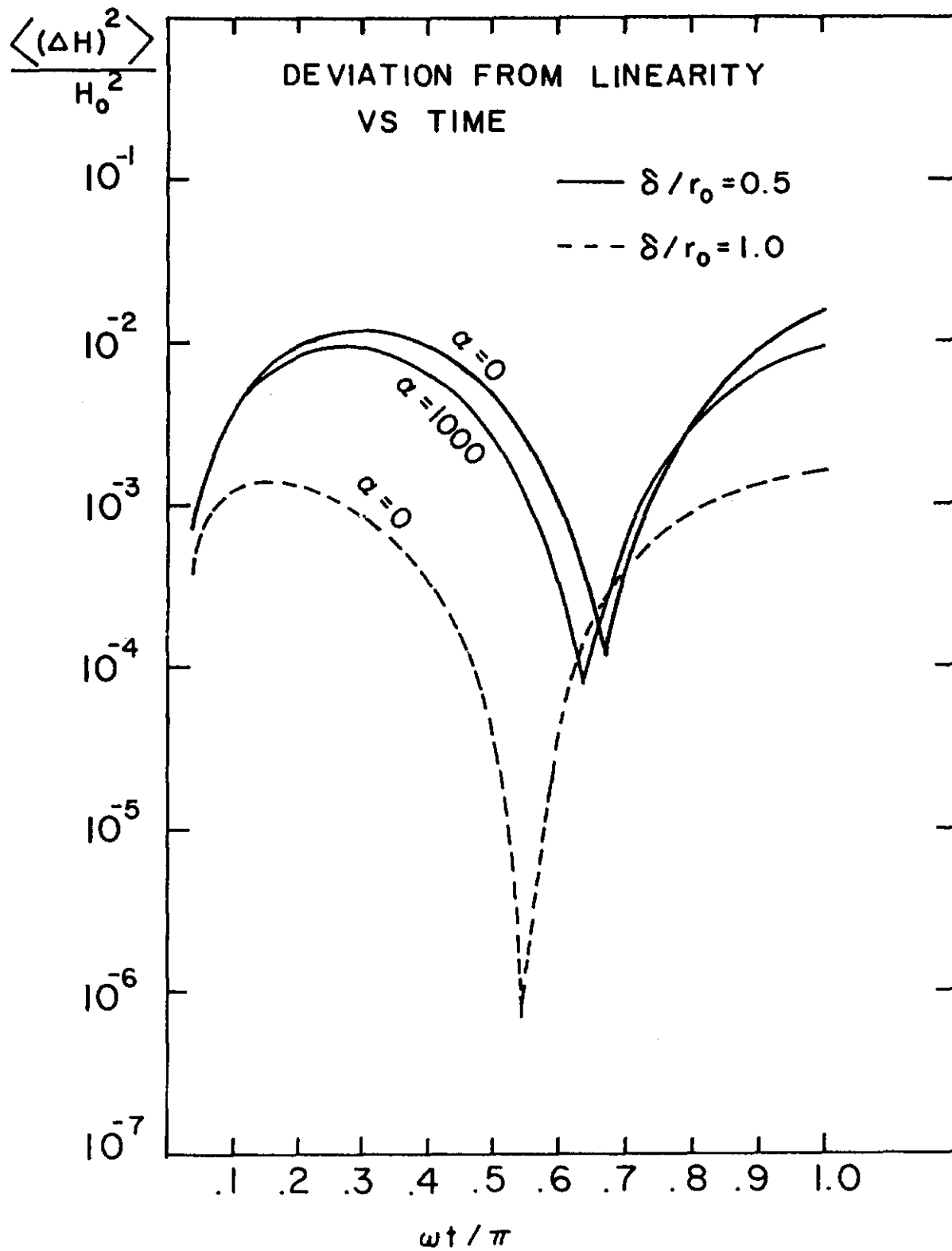


Fig. 3. A measure of the goodness of fit of the field to a straight line during the course of one pulse.

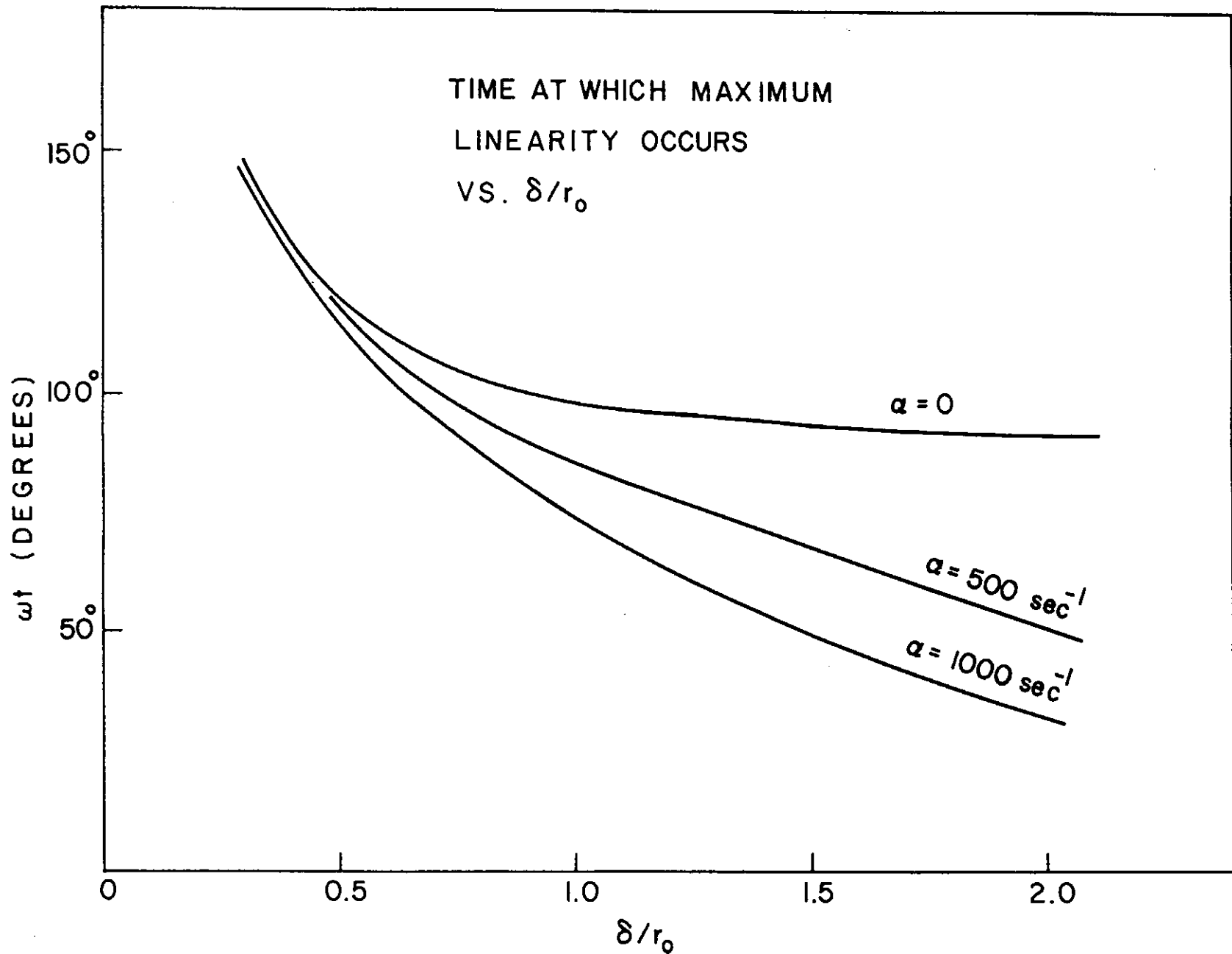


Fig. 4 The time during the pulse at which maximum linearity occurs. The pulse lasts for a time interval corresponding to $0 < \omega t < 180^\circ$.

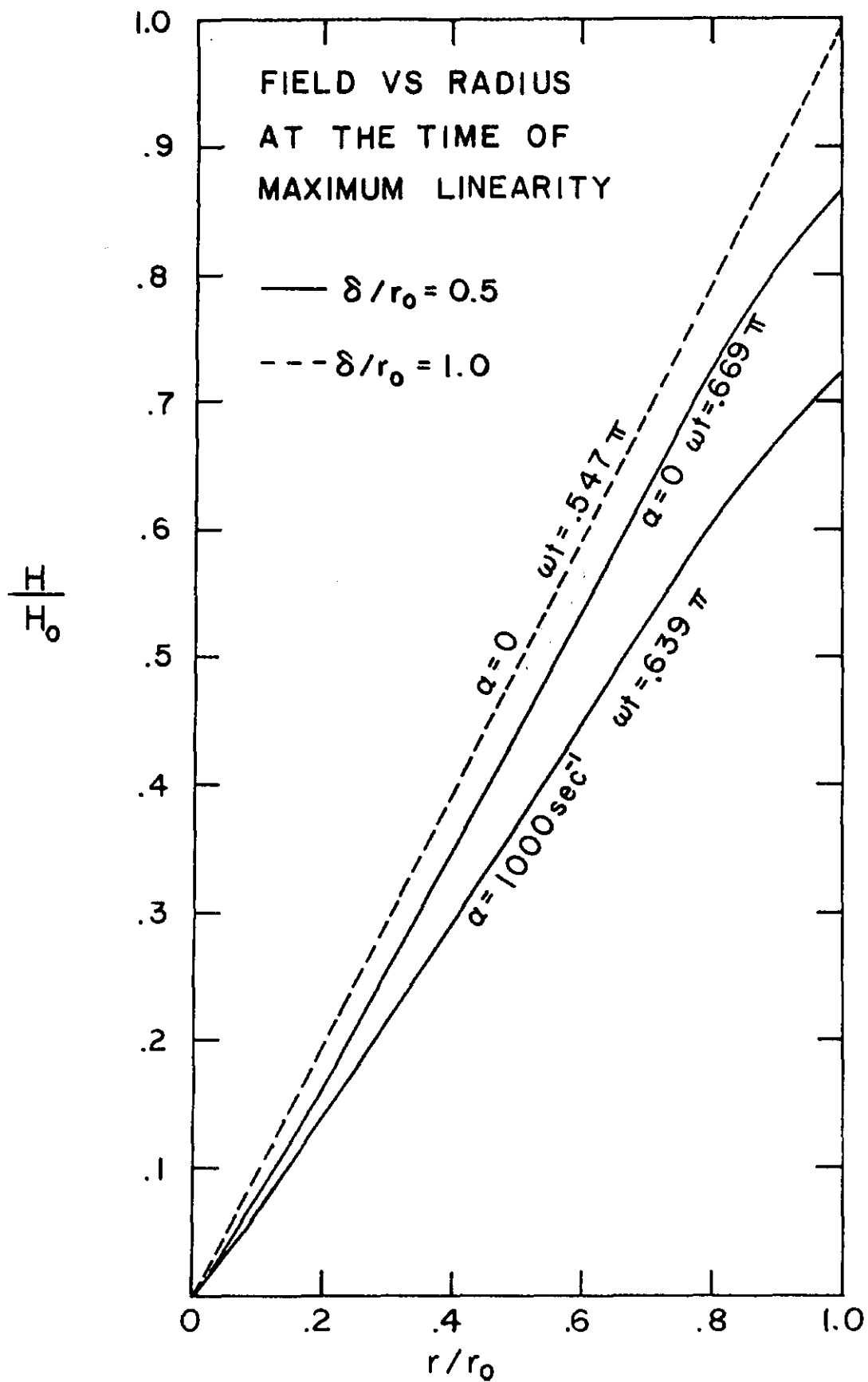


Fig. 5 Maximum achievable linearity for $\delta/r_0=0.5$ and 1.0 assuming the same value of H_0 for each curve.

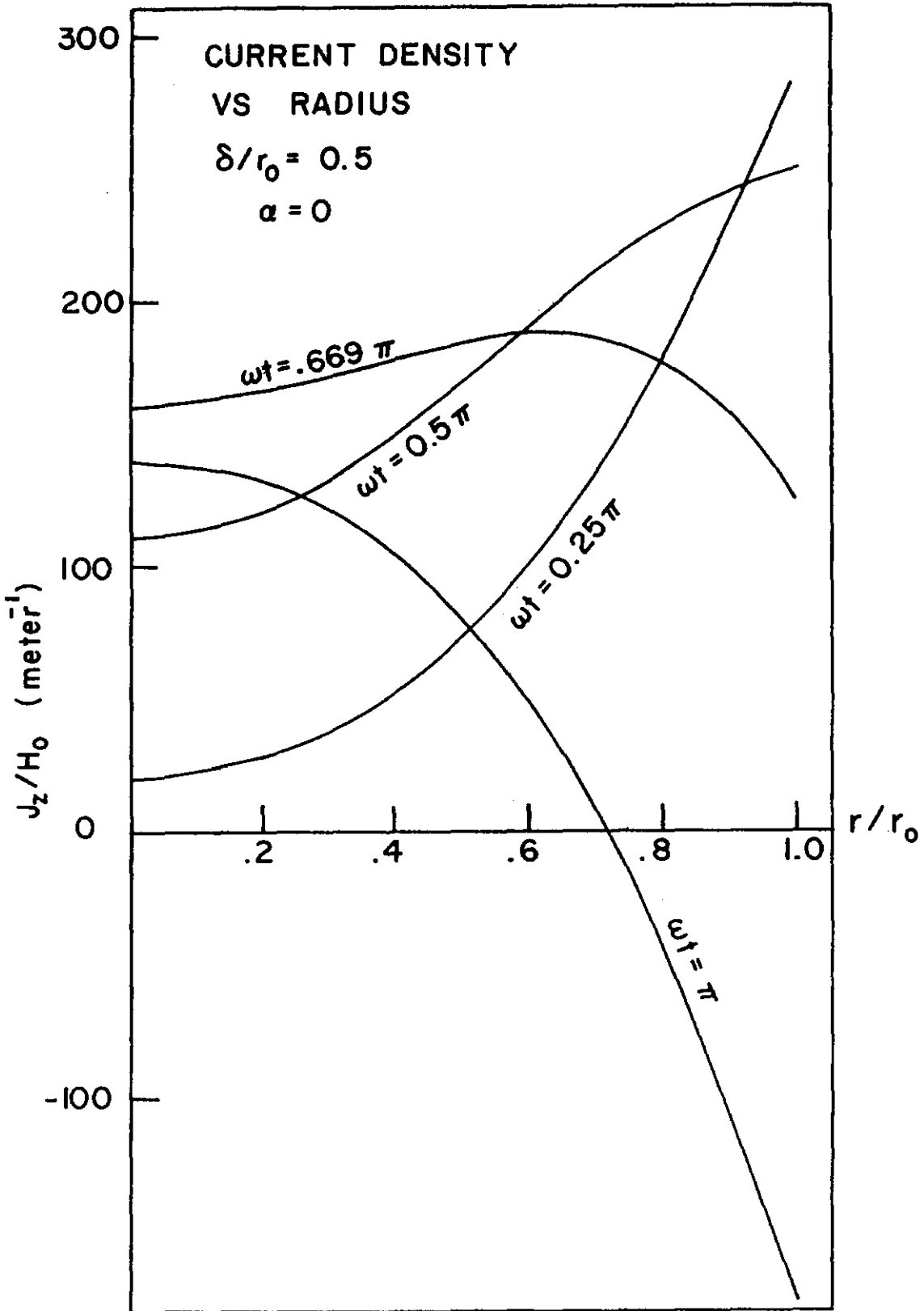


Fig. 6 Current density vs radius at various times during the pulse. The curve labeled $.669\pi$ corresponds to the maximum achievable linearity of the field.

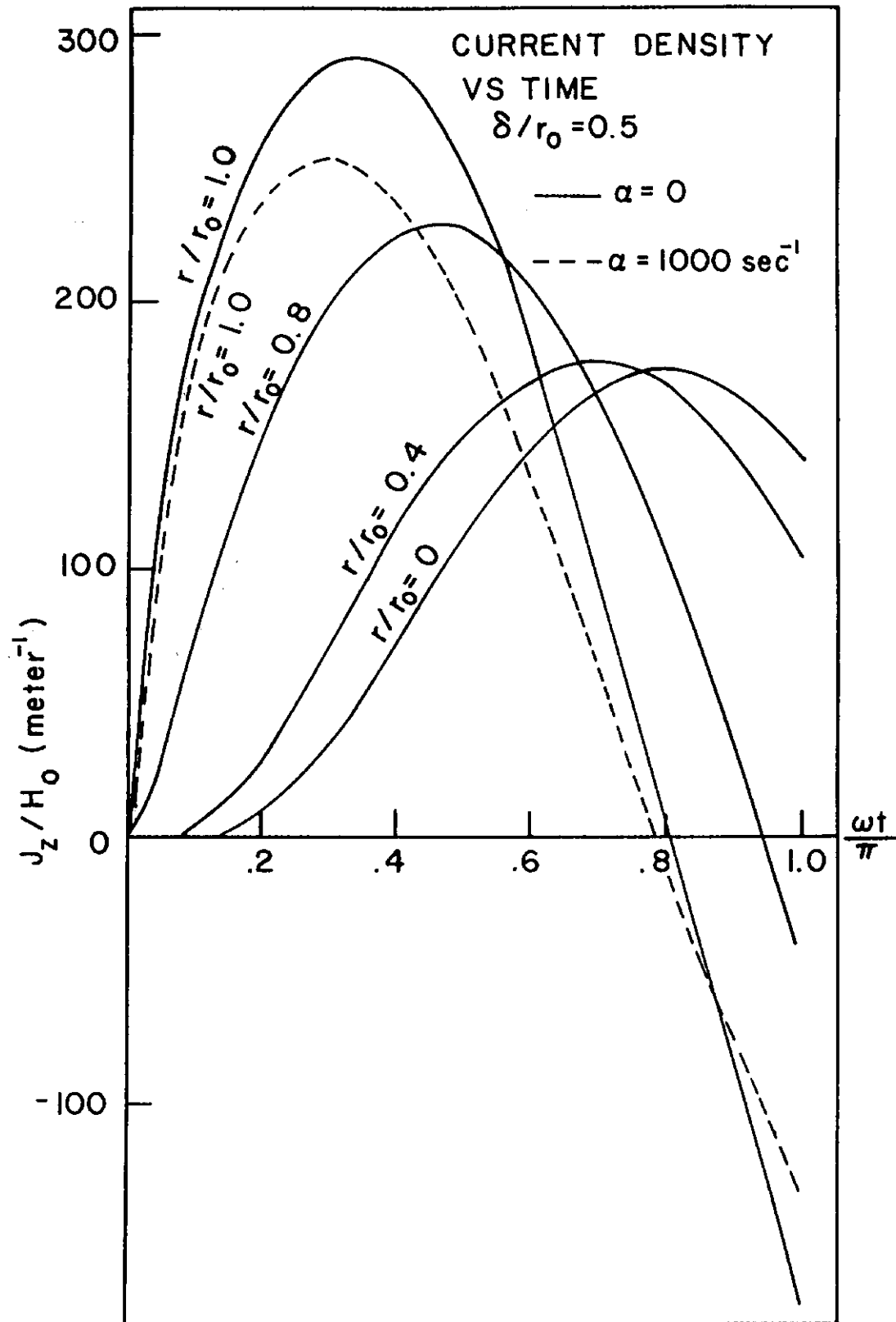


Fig. 7 Current density vs time at various distances from the axis. This figure contains the same information as Fig. 6.

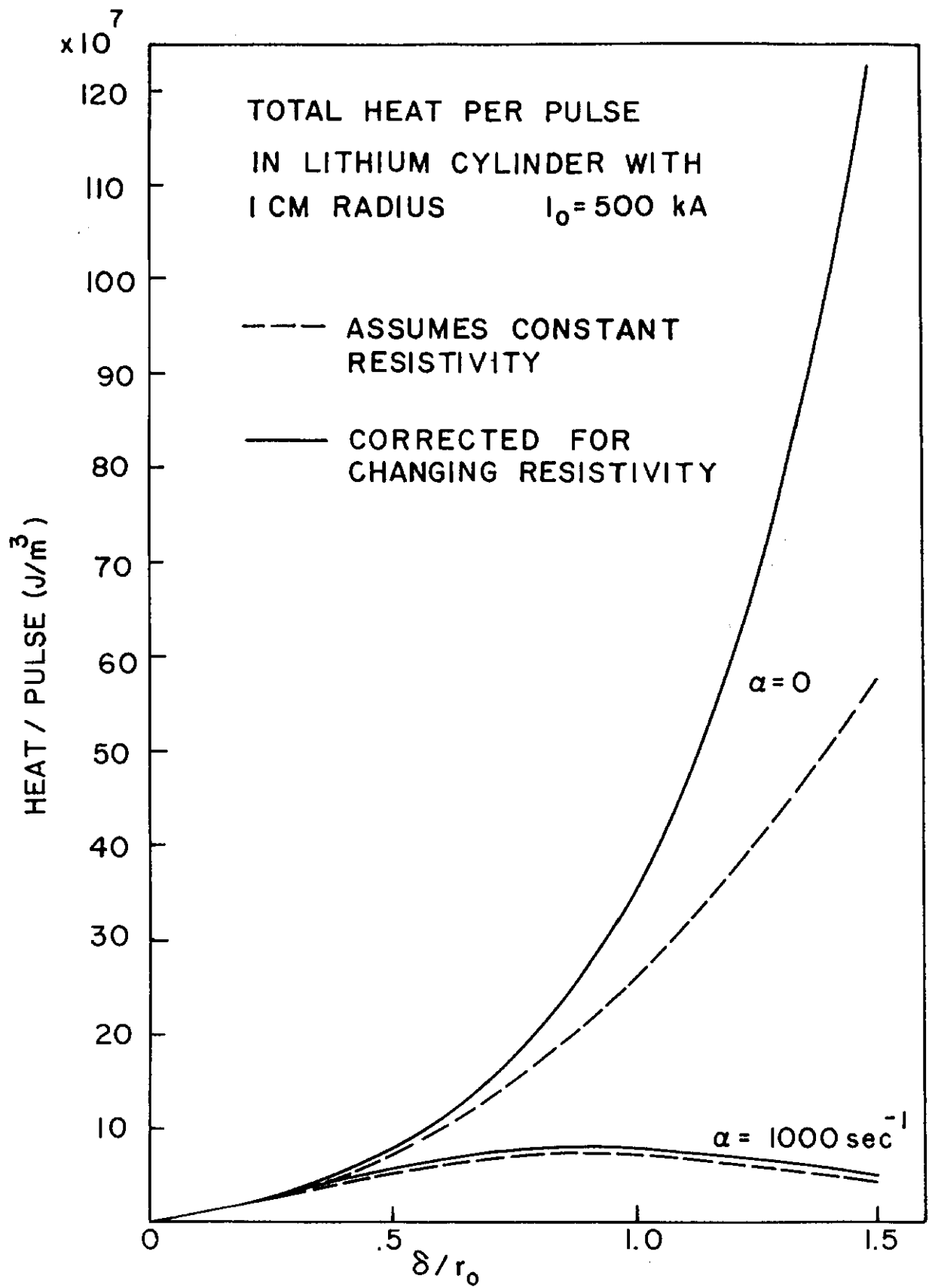


Fig. 8 Joule heat deposited during one pulse. See equations (28) and (29).

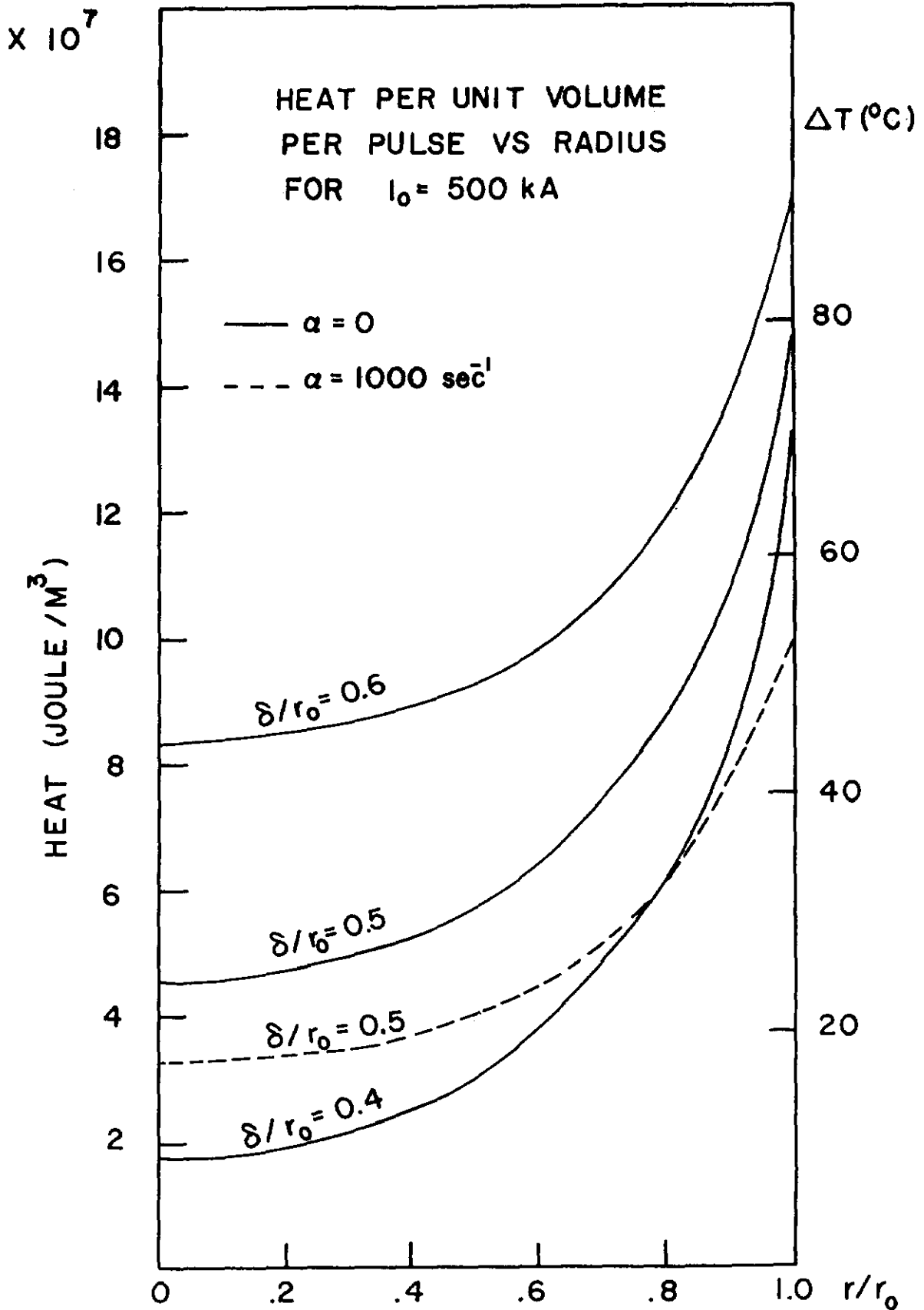


Fig. 9 Heat per unit volume per pulse vs radius for a lithium cylinder of radius 1.0 cm. The ΔT scale was calculated assuming $T=0^\circ\text{C}$ at the start of the pulse and $c_V=1.88 \times 10^6 \text{ Jm}^{-3}/^\circ\text{C}$.